

A pair natural orbital implementation of the coupled cluster model CC2 for excitation energies

Benjamin Helmich and Christof Hättig

Citation: J. Chem. Phys. **139**, 084114 (2013); doi: 10.1063/1.4819071
View online: http://dx.doi.org/10.1063/1.4819071
View Table of Contents: http://jcp.aip.org/resource/1/JCPSA6/v139/i8
Published by the AIP Publishing LLC.

Additional information on J. Chem. Phys.
Journal Homepage: http://jcp.aip.org/
Journal Information: http://jcp.aip.org/about/about_the_journal
Top downloads: http://jcp.aip.org/features/most_downloaded
Information for Authors: http://jcp.aip.org/authors

ADVERTISEMENT



A pair natural orbital implementation of the coupled cluster model CC2 for excitation energies

Benjamin Helmich[a] and Christof Hättig[b]
Lehrstuhl für Theoretische Chemie, Ruhr-Universität Bochum, 44801 Bochum, Germany

(Received 20 June 2013; accepted 8 August 2013; published online 30 August 2013)

We demonstrate how to extend the pair natural orbital (PNO) methodology for excited states, presented in a previous work for the perturbative doubles correction to configuration interaction singles (CIS(D)), to iterative coupled cluster methods such as the approximate singles and doubles model CC2. The original $\mathcal{O}(\mathcal{N}^5)$ scaling of the PNO construction is reduced by using orbital-specific virtuals (OSVs) as an intermediate step without spoiling the initial accuracy of the PNO method. Furthermore, a slower error convergence for charge-transfer states is analyzed and resolved by a numerical Laplace transformation during the PNO construction, so that an equally accurate treatment of local and charge-transfer excitations is achieved. With state-specific truncated PNO expansions, the eigenvalue problem is solved by combining the Davidson algorithm with deflation to project out roots that have already been determined and an automated refresh with a generation of new PNOs to achieve self-consistency of the PNO space. For a large test set, we found that truncation errors for PNO-CC2 excitation energies are only slightly larger than for PNO-CIS(D). The computational efficiency of PNO-CC2 is demonstrated for a large organic dye, where a reduction of the doubles space by a factor of more than 1000 is obtained compared to the canonical calculation. A compression of the doubles space by a factor 30 is achieved by a unified OSV space only. Moreover, calculations with the still preliminary PNO-CC2 implementation on a series of glycine oligomers revealed an early break even point with a canonical RI-CC2 implementation between 100 and 300 basis functions.
© *2013 AIP Publishing LLC*. [http://dx.doi.org/10.1063/1.4819071]

I. INTRODUCTION

Nowadays, an unbiased and sometimes even a qualitatively correct description of electronic excitations in large systems is still a challenging task for quantum chemistry. Indeed, arbitrary accuracy can be achieved with coupled cluster (CC) methods when orders in the perturbation are subsequently introduced through approximate CC models like in the hierarchy CCS (singles), CC2,[1] CCSD (singles and doubles), CC3,[2,3] ... up to arbitrary order.[4] However, application of higher-order CC response methods for excitation energies is still restricted to small molecules when standard computer hardware is used and calculations should not take more than a couple of days. For medium-sized systems with up to 1000 basis functions, the treatment of excited states with wave function based methods that are correct through second-order in perturbation give a decent description for single excitations out of a closed-shell ground state. For pronounced multi-reference cases, the complete active space perturbation theory through second-order[5] (CASPT2) accounts for both static and dynamic correlation. However, its application is limited to systems where only a few electrons are included in the active space due to the factorial scaling. Also, a simultaneous description of valence and Rydberg excitations is often problematic with CASPT2. Excited states of extended systems with more than 1000 basis functions can routinely be treated with time-dependent density functional theory (TDDFT) within the framework of response theory.[6,7] In general, density functional theory (DFT) lacks systematic improvability. In particular, TDDFT has with current standard functionals problems to accurately describe doubly excited states, Rydberg states, and charge-transfer (CT) excitations in extended systems.[8]

To extend the applicability of wave function based methods towards larger systems, versatile approximations have been introduced to reduce the computational costs. These approximate methods aim at an efficient, but still accurate, treatment of electron correlation and have in common that they exploit the locality of electron correlation in some sense, which, in principle, leads to linear scaling of all computational and storage resources with the system size. For the evaluation of the ground state correlation energy, approved strategies are based on, e.g., integral screening in the atomic orbital (AO) basis[9,10] and incremental schemes.[11,12] The latter approach was recently extended to the calculation of excitation energies, as well.[13]

A much more eminent compression of the number of wave function parameters is accomplished by the introduction of pair-specific virtual orbitals. Prominent examples are the domain-based local approach, which was initially proposed by Pulay and Saebø[14,15] and was later extensively applied to second-order Møller–Plesset perturbation theory[16] (MP2) and CC methods for the ground state[17,18] as well as excited states[19–21] by Werner and Schütz and their co-worker, respectively.

[a]Electronic mail: benjamin.helmich@rub.de
[b]Electronic mail: christof.haettig@rub.de

 © 2013 AIP Publishing LLC

Already in they 1970s, pair natural orbitals (PNOs) have been introduced to reduce the number of double excitations in correlated wave function calculations.[22–25] Despite their initial popularity, PNOs have fallen into oblivion for decades because the additional integral transformations into a pair-specific virtual basis emerged as a severe computational and storage bottleneck. Recently, it was demonstrated by Neese *et al*. for the coupled electron pair approximation (CEPA)[26] and CCSD[27] that the original limitations of the PNO approach can with today's computer hardware be circumvented by the resolution-of-the-identity (RI) approximation for two-electron integrals.[28,29] Moreover, Tew *et al*.[30,31] and Hättig *et al*.[32] showed how to use truncated PNO expansions for both the virtual and complementary auxiliary orbital space in explicitly correlated MP2 and MP3 calculations.

In the domain-based local approach, a set of predetermined projected atomic orbitals (PAOs) are generated by orthogonalizing the AOs against the occupied orbital space expressed in localized molecular orbitals (LMOs). Local orbital domains contain PAOs of a subset of atoms that lie in the spatial vicinity of a particular LMO and are then unified to pair domains if the two LMOs are spatially close to each other. Since the pair domains are determined without inspecting the electronic structure, they can be constructed efficiently. However, they exhibit a limited error control and the accuracy strongly depends on the appropriateness of the domain choices.

These problems can be avoided[33] with the recently introduced orbital-specific virtual (OSV) orbitals,[34] which are obtained either by a singular value decomposition of doubles amplitudes for diagonal pairs[34] or by minimization of the Hylleras functional.[35] For PNOs, a pair-specific virtual orbital space is generated right in the beginning by diagonalization of the pair contribution to the virtual-virtual block of the one-electron density matrix constructed from a first-order guess for the doubles amplitudes, which will be referred to as pair density. Compared to the OSV approximation, this results in a much more compact virtual space for non-diagonal pairs because redundancies from a unification of two orbital spaces are avoided. Optimization of a truncated virtual space rather on a pair-level (PNOs) than on an orbital-level (OSVs) necessitates additional computational efforts, which can be reduced significantly by using PAOs[36] or OSVs[32,37] intermediately during the PNO construction.

In a previous work,[38] we showed for the perturbative doubles correction[39] (D) to configuration interaction singles, CIS(D), that truncated PNO expansions can be easily applied to the treatment of excited states. Similar to the ground state, the excited state doubles amplitudes are expanded in their own truncated PNO bases, which are obtained from the analysis of a first-order guess for the doubles amplitudes. Using separate PNO expansions for the ground state and excited state doubles leads to a beneficial error compensation for the total PNO truncation error for CIS(D), which is always less than the separate errors in the ground state and excited state contributions to CIS(D). Additionally, we could show that for excited states the scaling of the number of PNOs in truncated expansions of the doubles with the system size is at worst linear like for the ground state, but even sub-linear if the electronic transition is restricted to sub-units of the molecule. This effect is promising for the application of PNOs to excited states of large molecules where often large parts of the molecule are not involved in the electronic transition.

In the current work, we present a first implementation of the non-perturbative CC2 model for excitation energies that is based on PNOs. We focus on three main issues: First, we discuss how to reduce the costs for the excited state PNO construction by adapting the hybrid OSV-PNO approach of Ref. 32 to excited states. This requires a modification of the OSV construction, which is discussed in Sec. III. Second, we show that the slower convergence of the PNO truncation errors for charge-transfer excitations in comparison to local excitations, which was observed in our previous work,[38] can be removed. The third and main aspect of the current work is the solution of the eigenvalue problem for excitation energies in state-specific PNO bases, which is an important prerequisite to extend the PNO and other local approaches for excited states beyond second-order methods for single excitation dominated transitions. In Sec. VIII, we present some numerical examples to validate the PNO implementation and demonstrate its efficiency.

II. ITERATIVE SECOND-ORDER METHODS

Several second-order methods for excited states can be derived from the approximate coupled cluster model[1] CC2. With the dressed Hamiltonian

$$\hat{H} = \exp(-T_1)\, H \exp(T_1), \tag{1}$$

which is similarity transformed by the exponential of the single excitation cluster operator T_1, the coupled cluster equations for CC2 can be written as

$$\Omega_{\mu_1} = \langle \mu_1 | \hat{H} + [\hat{H}, T_2] | \mathrm{HF} \rangle = 0, \tag{2}$$

$$\Omega_{\mu_2} = \langle \mu_2 | \hat{H} + [F, T_2] | \mathrm{HF} \rangle = 0. \tag{3}$$

These cluster equations with the vector function Ω_μ determine the amplitudes t_{μ_1} and t_{μ_2}, which appear either in $\hat{H}$ or in the double excitation cluster operator $T_2 = \sum_{\mu_2} t_{\mu_2} \tau_{\mu_2}$. The ground state energy is obtained as

$$E = \langle \mathrm{HF} | \hat{H} + [\hat{H}, T_2] | \mathrm{HF} \rangle. \tag{4}$$

Since the doubles equations are approximated to be correct through first order only, the CC2 energy is correct up to second order.

Within the framework of response theory, electronic excitation energies are obtained as the eigenvalues of the Jacobian matrix **A**. For CC2, the Jacobian exhibits the following form:

$$A^{\mathrm{CC2}}_{\mu\nu} = \frac{\partial \Omega^{\mathrm{CC2}}_{\mu}}{\partial t_\nu} = \begin{pmatrix} \langle \mu_1 | [\hat{H}, \tau_{\nu_1}] + [[\hat{H}, \tau_{\nu_1}], T_2] | \mathrm{HF} \rangle & \langle \mu_1 | [\hat{H}, \tau_{\nu_2}] | \mathrm{HF} \rangle \\ \langle \mu_2 | [\hat{H}, \tau_{\nu_1}] | \mathrm{HF} \rangle & \delta_{\mu_2\nu_2} \Delta_{\nu_2} \end{pmatrix}, \tag{5}$$

where $\Delta_{\mu_2} = \varepsilon_a + \varepsilon_b - \varepsilon_i - \varepsilon_j$ with canonical orbital energies ε_p. The Jacobian of the quasi-degenerate

second-order perturbation correction to single excitation configuration interaction,[40] CIS(D$_\infty$), can be obtained from $\mathbf{A}^{\mathrm{CC2}}$ by omitting the similarity transformation of the Hamiltonian with the t_{μ_1} amplitudes and the Jacobian of the algebraic diagrammatic construction through second order,[41] ADC(2), by symmetrizing the CIS(D$_\infty$) Jacobian,[42]

$$\mathbf{A}^{\mathrm{ADC(2)}} = \tfrac{1}{2}\left(\mathbf{A}^{\mathrm{CIS(D_\infty)}} + \mathbf{A}^{\mathrm{CIS(D_\infty)}\dagger}\right). \tag{6}$$

This symmetrization affects only the T_2-dependent contribution to the singles-singles block of the Jacobian $\langle\mu_1|[[\hat{H}, T_2], \tau_{\nu_1}]|\mathrm{HF}\rangle$, so that both, CIS(D$_\infty$) and ADC(2), can be implemented through simple modification of the CC2 Jacobian. Therefore, we discuss only the implementation of CC2 in the following.

Since only a few of the lowest excited states have practical relevance, it is common practice to compute the eigenvalues of the Jacobian with iterative methods, which necessitate the evaluation of matrix vector products,

$$\sigma_{\mu_i} = A_{\mu_i \nu_j}\, b_{\nu_j}, \tag{7}$$

where the Jacobian is transformed with trial vectors b_{μ_i} for the right eigenvectors.

In conventional CC2 implementations, the most time-consuming steps scale as $\mathcal{O}(\mathcal{N}^5)$ with the system size $\mathcal{N}$. The cost, though not the scaling, of a conventional CC2 calculation can be significantly reduced by using the RI approximation in combination with an on-the-fly generation of the integrals.[43] When similarity transformed integrals $(pq\hat{|}rs)$ are computed, the singles t_{μ_1} can be absorbed into the transformation matrices[44] from the AO to the molecular orbital (MO) basis

$$(pq\hat{|}rs) = \Lambda^p_{\alpha p}\Lambda^h_{\beta q}\Lambda^p_{\gamma r}\Lambda^h_{\delta s}(\alpha\beta|\gamma\delta), \tag{8}$$

$$\mathbf{\Lambda}^p = \mathbf{C}\left(\mathbf{1} - \mathbf{t}_\mathbf{1}^\mathbf{T}\right), \tag{9}$$

$$\mathbf{\Lambda}^h = \mathbf{C}(\mathbf{1} + \mathbf{t_1}), \tag{10}$$

where Greek letters denote AOs and $\mathbf{C}$ contains the canonical MO coefficients. The auxiliary matrix $\mathbf{t}_1$ is defined as[45]

$$\mathbf{t_1} = \begin{pmatrix} \mathbf{0} & \mathbf{0} \\ \{\mathbf{t_{ai}}\} & \mathbf{0} \end{pmatrix}. \tag{11}$$

Likewise, one-index transformed integrals $(ai\bar{|}bj)$, which are dressed with the singles part of the trial vectors b_{ai}, can be computed using the modified transformation matrices $\bar{\Lambda}^p_{\alpha a} = -C_{\alpha i}\, b_{ai}$ and $\bar{\Lambda}^h_{\alpha i} = C_{\alpha a}\, b_{ai}$

$$(ai\bar{|}bj) = \hat{P}^{ij}_{ab}\left(\bar{\Lambda}^p_{\alpha a}\Lambda^h_{\beta i} + \Lambda^p_{\alpha a}\bar{\Lambda}^h_{\beta i}\right)\Lambda^p_{\gamma b}\Lambda^h_{\delta j}(\alpha\beta|\gamma\delta). \tag{12}$$

The operator $\hat{P}^{ij}_{ab}$ symmetrizes a function $f_{ai,bj}$ in the index pairs (ai) and (bj), i.e., $\hat{P}^{ij}_{ab} = f_{ai,bj} + f_{bj,ai}$. For notational convenience, we will denote in the following two-electron integrals with two occupied and two virtual indices as $K^{ij}_{ab} = (ai|bj)$, $\hat{K}^{ij}_{ab} = (ai\hat{|}bj)$, and $\bar{K}^{ij}_{ab} = (ai\bar{|}bj)$.

Within the RI approximation, the two-electron integrals are rewritten as

$$(pq\hat{|}rs) = \sum_Q \hat{B}^Q_{pq}\hat{B}^Q_{rs}, \tag{13}$$

where Q is an auxiliary basis function for the RI approximation[43] and

$$\hat{B}^Q_{pq} = \Lambda^p_{\alpha p}\Lambda^h_{\beta q}(\alpha\beta|P)[\mathbf{V}^{-1/2}]_{PQ} \tag{14}$$

with $V_{PQ} = (P|Q)$. Similarly, the barred integrals are approximated by

$$\bar{K}^{ij}_{ab} = \hat{P}^{ij}_{ab}\sum_Q \bar{B}^Q_{ai}\hat{B}^Q_{bj} \tag{15}$$

with

$$\bar{B}^Q_{pq} = \left(\bar{\Lambda}^p_{\alpha a}\Lambda^h_{\beta i} + \Lambda^p_{\alpha a}\bar{\Lambda}^h_{\beta i}\right)(\alpha\beta|P)[\mathbf{V}^{-1/2}]_{PQ}. \tag{16}$$

III. HYBRID OSV-PNO APPROACH FOR EXCITED STATES

Truncated PNO expansions scale linearly with the system size as it was previously demonstrated for electronic ground[25,26] and excited states.[38] However, the computation of PNOs from pair densities in a canonical virtual basis is still an $\mathcal{O}(\mathcal{N}^5)$-scaling step, which would limit the applicability of PNO methods to medium-sized molecules. As it was recently demonstrated by Krause and Werner[37] and Hättig *et al.*,[32] the scaling of the PNO construction can be reduced by one order when pair densities are built in a unified OSV basis. Following this strategy, the PNO construction can be further accelerated by calculating the OSVs via an iterative diagonalization procedure as proposed by Schmitz *et al.*[47] Combining the iterative diagonalization with a local version of the RI approximation for two-electron integrals results in a PNO implementation with $\mathcal{O}(\mathcal{N}^2)$-scaling costs.

The introduction of a set of ground state OSVs $\tilde{a}$ (GS-OSVs) for each LMO i leads to a local approximation for the three-index intermediates B^Q_{ai} that enter the exchange integrals in the numerator of the amplitudes

$$t^{ij}_{ab} = \frac{K^{ij}_{ab}}{F_{ii} - \varepsilon_a + F_{jj} - \varepsilon_b}. \tag{17}$$

In the last equation, F_{ii} are the diagonal elements of the Fock matrix in the LMO basis. This approximation is sufficiently accurate for ground states if the OSVs are obtained from the eigenvectors of the doubles amplitudes for the diagonal pairs t^{ii}_{ab}. However, excited state OSVs (ES-OSVs) for a LMO i must be suitable to approximate both $\hat{B}^Q_{ai}$ and $\bar{B}^Q_{ai}$, which enter the barred exchange integrals $\bar{K}^{ij}_{ab}$ in the numerator of the first-order excited state amplitudes,

$$b^{ij}_{ab} = \frac{\bar{K}^{ij}_{ab}}{F_{ii} - \varepsilon_a + F_{jj} - \varepsilon_b + \omega}, \tag{18}$$

where ω is an approximate excitation energy. Constructing the ES-OSVs from the amplitudes for the diagonal pairs b^{ii}_{ab} in Eq. (18) analogously to GS-OSVs will not lead to a reasonable approximation for all off-diagonal pairs. If a LMO i is not involved in the excitation process, the amplitudes b^{ii}_{ab} are negligible and lead to very few OSVs $\tilde{a}_i$ with significant occupation numbers. For off-diagonal pairs where the second LMO j is involved in the excitation process, such OSVs $\tilde{a}_i$

are not suitable to approximate $\hat{B}^Q_{ai}$ in $\bar{K}^{ij}_{ab}$ because, then, $\bar{K}^{ij}_{ab}$ vanishes. A more appropriate set of ES-OSVs is obtained by diagonalizing modified amplitudes

$$b'^{ii}_{ab} = \frac{\hat{B}^Q_{ai}\,\hat{B}^Q_{bi} + \bar{B}^Q_{ai}\,\bar{B}^Q_{bi}}{2F_{ii} + \omega - \varepsilon_a - \varepsilon_b}, \tag{19}$$

which are also positive semi-definite, similar to the ground-state first-order amplitudes for diagonal pairs. The choice in Eq. (19) is not unique. We also investigated a higher-order singular value decomposition[48,49] (HOSVD) of four amplitude-like matrices computed from the integrals $\hat{B}^Q_{ai}\,\hat{B}^Q_{bi}$, $\bar{B}^Q_{ai}\,\hat{B}^Q_{bi}$, $\hat{B}^Q_{ai}\,\bar{B}^Q_{bi}$, and $\bar{B}^Q_{ai}\,\bar{B}^Q_{bi}$. This leads, however, only to a slightly improved accuracy compared to the diagonalization of b'^{ii}_{ab}. Therefore, we decided to determine OSVs for excited states from the modified amplitudes in Eq. (19), which has slightly lower computational costs. From a conceptional point of view, this procedure is similar to that used in the domain-based local methods for exited states, which was initially proposed by Korona and Werner.[19] In their approach, orbital domains are chosen as union of ground state LMOs and excited orbital domains obtained from the analysis of a guess for the singles part of the excitation vector.

An initial (excited state) pre-PNO basis for a pair ij is then constructed by merging the ES-OSVs for the LMOs i and j.[32] This pre-PNO basis is, however, only constructed if a spin-opposite scaled (SOS) like estimate for the pair contribution to the excited state doubles contribution ω_{es} to the CIS(D) excitation energy in the direct OSV approximation,[34]

$${}^{\mathrm{SOS}}\omega^{ij}_{es} = \frac{c_{os}}{4}\frac{\left(\bar{K}^{ij}_{\tilde{a}_i\tilde{b}_j}\right)^2}{\omega + F_{ii} + F_{jj} - F_{\tilde{a}_i\tilde{a}_i} - F_{\tilde{b}_j\tilde{b}_j}}, \tag{20}$$

is above a pair threshold T_{pair}. $\bar{K}^{ij}_{\tilde{a}_i\tilde{b}_j}$ are the barred integrals in the direct OSV approximation and $F_{\tilde{a}_i\tilde{a}_i}$ the diagonal elements of the virtual-virtual block of the Fock matrix in the OSV basis of LMO i. After constructing a pre-PNO basis, a truncated PNO basis is obtained by a procedure outlined in Ref. 38 from the eigenvectors of pair densities $\mathbf{D}^{ij} = (2\mathbf{b}^{ij} - \mathbf{b}^{ij\dagger})^\dagger\mathbf{b}^{ij} + (2\mathbf{b}^{ij} - \mathbf{b}^{ij\dagger})\mathbf{b}^{ij\dagger}$ computed from first-order excited state amplitudes (cmp. Eq. (18)), $b^{ij}_{\tilde{a}_{ij}\tilde{b}_{ij}}$, in the pre-PNO basis $\tilde{a}_{ij}$, $\tilde{b}_{ij}$ for pair ij.

IV. IMPLEMENTATION OF PNO-CC2

Doubles amplitudes expanded in a limited number of PNOs as well as exchange type integrals with two occupied and two PNO indices $K^{ij}_{\tilde{a}\tilde{b}}$ scale linearly with the system size and can be efficiently computed and stored on disk. In the present implementation, the construction of the OSV basis still scales as $\mathcal{O}(\mathcal{N}^4)$ because of the diagonalization of doubles amplitudes for diagonal pairs in a full virtual basis. Currently, we also accept cubically and quartically scaling steps for intermediates that can be computed in close analogy to the RI-CC2 implementation described in Ref. 43. We note, however, that with the techniques proposed in Ref. 47 the scaling can be further reduced to $\mathcal{O}(\mathcal{N}^2)$, which will be subject of future work.

TABLE I. Explicit expressions and formal cost-scaling in the canonical RI-CC2 and the PNO-CC2 implementation for the Jacobian transformed vectors $\sigma_{ai} = \sigma^0_{ai} + \sigma^H_{ai} + \sigma^I_{ai} + \sigma^{JG}_{ai}$ and $\sigma^{ij}_{\tilde{a}\tilde{b}} = \sigma^E_{\tilde{a}i\tilde{b}j} + \sigma^F_{\tilde{a}i\tilde{b}j}$. A tilde on top of a four-index term denotes $\tilde{X}^{ij}_{\tilde{a}\tilde{b}} = 2X^{ij}_{\tilde{a}\tilde{b}} - X^{ij}_{\tilde{b}\tilde{a}}$.

	Scaling	
Step	RI-CC2	PNO-CC2
$E_{ji} = F_{ji} + \Lambda^p_{\alpha j}\Omega^{JG}_{\alpha i}$	N^3	
$E_{ab} = \hat{F}_{ab} - d^{ij}_{a\tilde{a}}\,\tilde{t}^{ij}_{\tilde{a}\tilde{c}}\,K^{ij}_{\tilde{b}\tilde{c}}\,d^{ij}_{b\tilde{b}}$	N^5	N^4
$\sigma^0_{ai} = E_{ab}\,b_{bi} + b_{aj}\,E_{ji}$	N^3	
$\bar{F}_{ia} = d^{ij}_{a\tilde{a}}\,\tilde{K}^{ij}_{\tilde{a}\tilde{b}}\,d^{ij}_{b\tilde{b}}\,b_{bj}$	N^4	N^2
$\sigma^I_{ai} = d^{ik}_{a\tilde{a}}\,\tilde{b}^{ik}_{\tilde{a}\tilde{c}}\,d^{ik}_{c\tilde{c}}\,\hat{F}_{kc} + d^{ik}_{a\tilde{a}}\,\tilde{t}^{ik}_{\tilde{a}\tilde{c}}\,d^{ik}_{c\tilde{c}}\,\bar{F}_{kc}$	N^4	N^2
$B^Q_{\tilde{a}_{ij}i} = B^Q_{ai}\,d^{ij}_{a\tilde{a}}$	–	N^3
$\bar{Y}^Q_{\tilde{a}_{ik}i} = \tilde{b}^{ik}_{\tilde{a}\tilde{c}}\,B^Q_{\tilde{c}_{ik}k}$	N^5	N^2
$\bar{Y}^Q_{ai} = d^{ik}_{a\tilde{a}}\,Y^Q_{\tilde{a}_{ik}i}$	–	N^3
$\bar{i}^Q = B^Q_{kc}\,b_{kc}$	N^3	
$\bar{\Gamma}^P_{i\beta} = \{\bar{Y}^Q_{ai}\,\Lambda^h_{\beta a} + 2\Lambda^h_{\beta i}\bar{i}^Q - \Lambda^h_{\beta c}\,b_{ck}\,\hat{B}^Q_{ki}\}[\mathbf{V}^{-1/2}]_{PQ}$	N^3	
$\sigma^H_{ai} = -\bar{Y}^Q_{ak}\,\hat{B}^Q_{ik}$	N^4	
$\sigma^{JG}_{ai} = \Lambda^p_{\alpha a}\,\bar{\Gamma}^P_{i\beta}(P\|\alpha\beta)$	N^3	
$\sigma^E_{\tilde{a}i\tilde{b}j} = \hat{P}^{ij}_{\tilde{a}\tilde{b}}\left(\varepsilon_{\tilde{a}_{ij}}\,b^{ij}_{\tilde{a}\tilde{b}} - F_{ik}S^{ij,kj}_{\tilde{a}\tilde{c}}\,b^{kj}_{\tilde{c}\tilde{d}}S^{ij,kj}_{\tilde{b}\tilde{d}}\right)$	N^4	N
$\sigma^F_{\tilde{a}i\tilde{b}j} = \bar{K}^{ij}_{\tilde{a}\tilde{b}} = \hat{P}^{ij}_{\tilde{a}\tilde{b}}\,\hat{B}^Q_{\tilde{a}_{ij}i}\,\bar{B}^Q_{b_{ij}j}$	N^5	N^2

Intermediates for the contraction of the Jacobian with a trial vector from the right are compiled in Table I. Explicit expressions for intermediates of the vector function and Jacobian transformed trial vectors are similar by construction.[43] Therefore, we limit a more detailed discussion to the computation of the Jacobian transformed trial vectors. In the current implementation of PNO-CC2, the computation of the global intermediates E_{ji}, with $\Omega^{JG}_{\alpha i} = \Gamma^P_{\beta i}(P|\alpha\beta)$, and E_{ab} scales with $\mathcal{O}(\mathcal{N}^3)$ and $\mathcal{O}(\mathcal{N}^4)$, respectively, due to construction of a similarity transformed Fock matrix. For second-order methods with no singles amplitudes, i.e., CIS(D), CIS(D_∞), and ADC(2), the global intermediates E_{ji} and E_{ab} can be evaluated with linear and cubic scaling, respectively.[38] But, the computation of these global intermediates is done only once and has a small pre-factor. Their contraction with the singles trial vectors to σ^0_{ai} (cmp. Table I) scales cubically and has a very small pre-factor.

In the current implementation, the three-index integrals in the PNO basis $\bar{B}^Q_{\tilde{a}i}$ are still computed by transforming $\bar{B}^Q_{ai}$ from the canonical virtual to the PNO basis. The initial computation of $\bar{B}^Q_{ai}$ in the canonical basis is a $\mathcal{O}(\mathcal{N}^4)$ step and currently dominates the costs together with the transformation of $\bar{Y}$ from the PNO to the canonical virtual basis and the construction of $\bar{\Gamma}^P_{i\beta}$, which are cubically and quartically scaling steps with sizeable pre-factors.

In contrast to this, the contractions and transformations that are already done fully in the PNO basis like the contraction of the integral intermediates $\hat{B}$ and $\bar{B}$ to exchange integrals $\bar{K}^{ij}_{\tilde{a}\tilde{b}}$ and the contraction of doubles amplitudes with three-index integrals to the $\bar{Y}$ intermediate in the PNO basis are performed with a quadratic cost-scaling. They are the dominant $\mathcal{O}(\mathcal{N}^5)$-scaling steps in the canonical RI-CC2

calculation, but contribute in the (preliminary) PNO implementation only a small fraction to the overall timings.

V. CHARGE-TRANSFER EXCITATIONS

In our previous work,[38] we observed that, compared to locally excited (LE) states, CT states exhibit PNO truncation errors that are slightly more pronounced and converge slower with decreasing T_{PNO}. However, the convergence is also for CT states as rapid as for LE states when for the construction of the truncated PNO basis the excited state doubles amplitudes are evaluated either in the canonical MO basis or with LMOs and a numerical Laplace transformation of the orbital energy denominators,[50,51]

$$b^{ij}_{\tilde{a}\tilde{b}} = \int_0^\infty dt \sum_{i'aj'b} X_{ii'}\, Y_{\tilde{a}a}\, \bar{K}^{i'j'}_{ab}\, X_{jj'}\, Y_{\tilde{b}b} \tag{21}$$

$$\approx \hat{P}^{ij}_{\tilde{a}\tilde{b}} \sum_{Qz} w_z \left(\sum_{i'a} \hat{B}^{Q}_{ai'} X^z_{ii'} Y^z_{\tilde{a}a} \right) \left(\sum_{j'b} \bar{B}^{Q}_{bj'} X^z_{jj'} Y^z_{\tilde{b}b} \right), \tag{22}$$

$$X^{(z)}_{ii'} = T_{ij}\, e^{-(\varepsilon_j + \frac{\omega}{4})t_{(z)}}\, T_{i'j}, \tag{23}$$

$$Y^{(z)}_{\tilde{a}a} = d^{ij}_{a\tilde{a}} e^{(\varepsilon_a - \frac{\omega}{4})t_{(z)}}, \tag{24}$$

where w_z and t_z are the Laplace weights and exponents, respectively, T_{ij} is the transformation matrix between LMOs and canonical MOs, and $d^{ij}_{a\tilde{a}}$ are the pre-PNO coefficients in the canonical MO basis a. Both approaches avoid the neglect of off-diagonal Fock matrix elements, which we will refer to as diagonal approximation.

The diagonal approximation, which is unproblematic for the construction of PNOs for ground and LE states, is the major source of error for CT states. For a better understanding of its origin, we analyzed the contribution from the excited state doubles amplitudes ω_{es} in the PNO basis to the doubles correction (D) in CIS(D). As a simple model system, we choose a complex of ethylene and tetrafluoroethylene separated by 12 a.u.[52] As shown in Fig. 1, the HOMOs and LUMOs of the two monomers correspond to the most dominant natural transition orbitals[53,54] (NTOs) for the transitions that we analyzed. For the excitations within (LE) and between the monomers (CT), the truncation error of ω_{es} is shown for different PNO truncation thresholds in Fig. 2. For both CT states, the truncation error of ω_{es} converges slowly and remains larger than 0.001 eV, even when tight thresholds ($-\log(\mathrm{T_{PNO}}) = 9, 10$) are employed. In contrast to this, the two LE states converge smoothly with T_{PNO}. Applying the numerical Laplace transformation reduces the truncation errors of both LE and CT excited states, for the latter by two to three orders of magnitude for $-\log(\mathrm{T_{PNO}}) = 8, \ldots, 10$.

This behavior is a consequence of a different convergence of the natural occupation numbers $n^{ij}_{\tilde{a}}$ for the CT excitations. The pairs that contribute significantly to ω_{es} can be divided into two groups. One contains pairs where both LMOs are in the spatial vicinity of the occupied NTO. The other group contains pairs where one LMO is close to the occupied NTO and the other close to the virtual NTO. The convergence of $n^{ij}_{\tilde{a}}$ is shown in Fig. 3 for one selected pair of each group. Pairs where both LMOs are spatially close to the occupied NTO have a few occupation numbers that are much larger than the remaining ones. For these pairs, the large difference between the most dominant and the less dominant occupation numbers can be explained qualitatively by a rank analysis of the dressed integrals $\bar{K}^{ij}_{ab}$ in the numerator of the doubles amplitudes. For distinct singly excited CT states, the electronic transition can be qualitatively described by a single pair of NTOs,

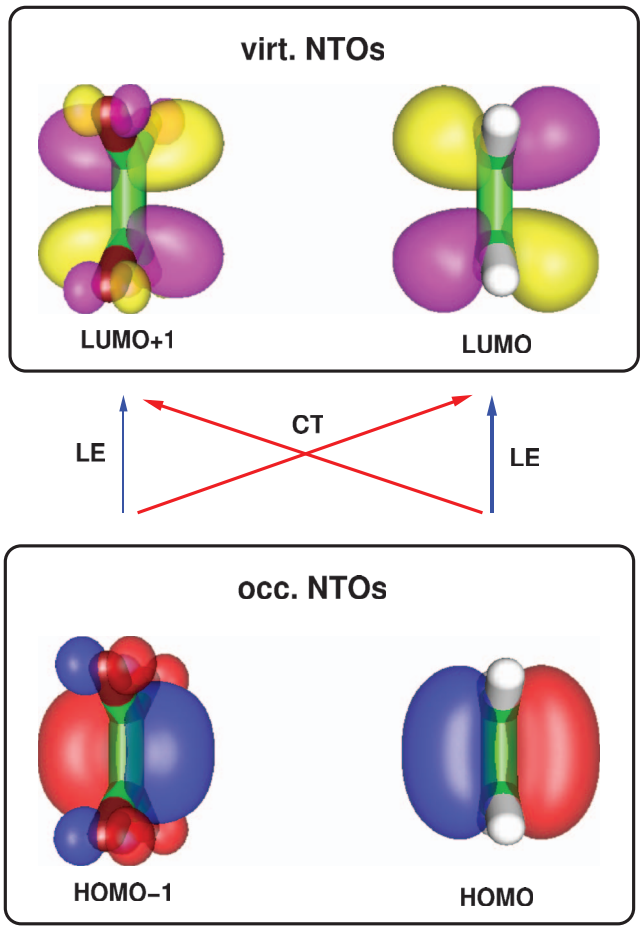


FIG. 1. The most significant occupied and virtual natural transition orbital (NTO) involved in the local (HOMO → LUMO, HOMO-1 → LUMO+1) and CT excitations (HOMO → LUMO+1, HOMO-1 → LUMO) of a $C_2H_4 - C_2F_4$ complex.

$$b_{ai} \approx \beta_{a\sigma^v}\, \beta_{i\sigma^o}, \tag{25}$$

with a singular value close to one. Applying this rank-one approximation of the excited state singles amplitudes to $\bar{K}^{ij}_{ab}$ leads to rank-V[55] and rank-one terms

$$\bar{K}^{ij}_{ab} \approx \hat{P}^{ij}_{ab} \{ \beta_{i\sigma^o} (a\sigma^v|bj) - \beta_{a\sigma^v} (\sigma^o i|bj) \}. \tag{26}$$

The rank-V terms $\hat{P}^{ij}_{ab} \beta_{i\sigma^o} (a\sigma^v|bj)$ contribute to $\bar{K}^{ij}_{ab}$ if one of the LMOs is close to the occupied NTO σ^o, i.e., if $\beta_{i\sigma^o}$ or $\beta_{j\sigma^o}$ is non-negligible, and the other is close to the virtual NTO σ^v so that $(a\sigma^v|bj)$ or $(ai|b\sigma^v)$ is non-vanishing. The rank-one terms contribute to $\bar{K}^{ij}_{ab}$ if at least one of the LMOs is close to the occupied NTO σ^o so that the integrals $(\sigma^o i|bj)$

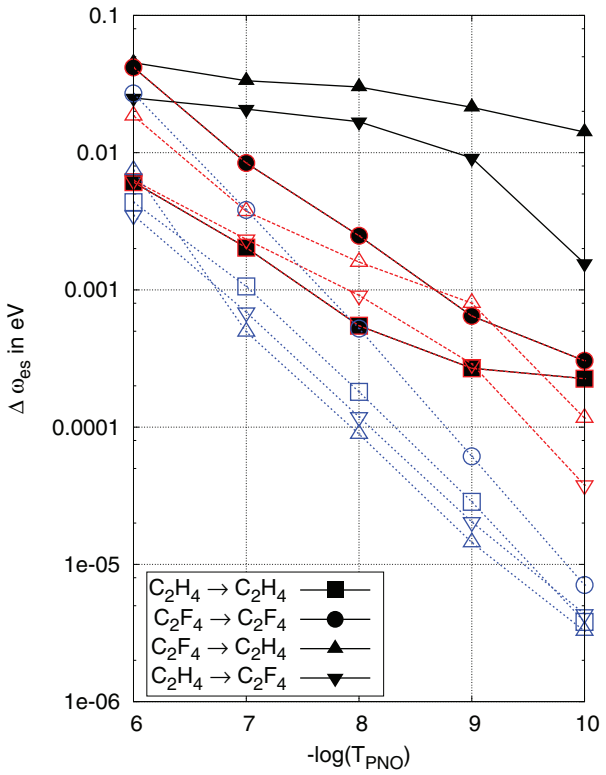


FIG. 2. PNO truncation errors of the excited state part to the doubles correction ω_{es} in CIS(D)/cc-pVDZ calculations for HOMO-LUMO local and CT excitations with different PNO truncation thresholds T_{PNO} in a C_2H_4–C_2F_4 complex separated by 12 a.u. Numerical Laplace integration was used for the PNO construction of either no (black), according to Eq. (30) selected (red), or all pairs (blue).

or $(ai|\sigma^o j)$ are non-vanishing. For LE states, both the rank-V and the rank-one terms are non-negligible for the same pairs. However, for CT states σ^o and σ^v are spatially separated from each other and the rank-V contributions become negligible for pairs where both i and j are close to the occupied MO. For these, one obtains $\bar{K}^{ij}_{ab}$ with at most two dominant singular values and pair densities with very few dominant eigenvalues. Thus, decreasing the PNO threshold mainly increases the number of PNOs for those pairs that contribute with rank-V terms while the number of PNOs of pairs that contribute only with rank-one terms remains essentially unchanged. As a consequence of this, the errors introduced at the level of the PNO construction by the diagonal approximation decrease only slowly for such pairs and dominate the PNO truncation error. Thus, just for pairs that contribute only through rank-one terms it is necessary to employ the numerical Laplace transformation to compute the pair contribution to the excited state doubles amplitudes in the LMO basis during the PNO construction without the diagonal approximation.

For second-order methods, the construction of the amplitudes during the PNO construction is one of the most time-consuming steps and its costs increase linearly with the number of Laplace quadrature points. It is, therefore, important to pre-select pairs where the diagonal approximation is replaced by the numerical Laplace transformation. These "Laplace pairs" are identified when the OSVs are merged to the pre-PNO basis. Here, it can be exploited that for distinct CT states both $\bar{K}^{ij}_{\tilde{a}\tilde{b}}$ and $b^{ij}_{\tilde{a}^i\tilde{b}^j}$ have very few dominant singular values $\tau^{ij}_{\tilde{c}}$,

$$b^{ij}_{\tilde{a}^i\tilde{b}^j} = U_{\tilde{a}^i\tilde{c}}\,\tau^{ij}_{\tilde{c}}\,V_{\tilde{b}^j\tilde{c}}, \tag{27}$$

if both LMOs are in the vicinity of the occupied NTO. Within the direct OSV approximation for the amplitudes $b^{ij}_{\tilde{a}^i\tilde{b}^j}$, we can estimate with negligible costs the contribution of individual OSVs to the energy estimate ${}^{\mathrm{SOS}}\omega^{ij}_{es}$, which is used to pre-select pairs for the PNO construction (see Sec. III)

$$\bar{K}^{ij}_{\tilde{c}} = U_{\tilde{a}^i\tilde{c}}\,\bar{K}^{ij}_{\tilde{a}\tilde{b}}\,V_{\tilde{b}^j\tilde{c}}, \tag{28}$$

$${}^{\mathrm{SOS}}\omega^{ij}_{es} = (1+\delta_{ij}c_{os})\,\bar{K}^{ij}_{\tilde{c}}\,\tau^{ij}_{\tilde{c}}. \tag{29}$$

Fig. 4 shows the convergence of ${}^{\mathrm{SOS}}\omega^{ij}_{es}$ for the two selected pairs of Fig. 3. If two OSVs are sufficient to recover at least $\alpha_{Lap}\%$ of ${}^{\mathrm{SOS}}\omega^{ij}_{es}$ and, at the same time, ${}^{\mathrm{SOS}}\omega^{ij}_{es}$ is larger than T_{Lap}, the amplitudes for this pair are evaluated through the numerical Laplace transformation, Eq. (21), in the subsequent PNO construction step. Test calculations revealed

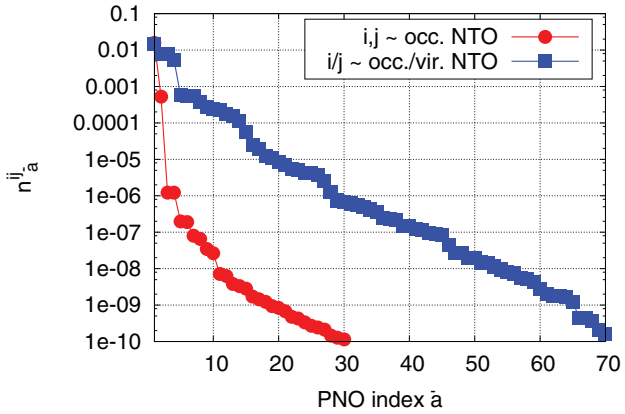


FIG. 3. Natural occupation numbers $n^{ij}_{\tilde{a}}$ for selected pairs of the $C_2H_4 \rightarrow C_2F_4$ HOMO-LUMO CT excitation. For one pair, both LMOs are close to the occupied NTO (red); for another pair, one LMO is close to the occupied and another LMO is close to the virtual NTO (blue).

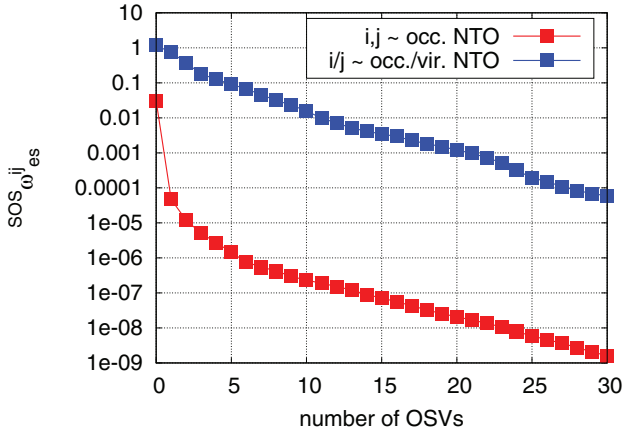


FIG. 4. Convergence of ${}^{\mathrm{SOS}}\omega^{ij}_{es}$ with the number of OSVs for selected pairs of the $C_2H_4 \rightarrow C_2F_4$ HOMO-LUMO CT excitation. For one pair, both LMOs are close to the occupied NTO (red); and for another pair, one LMO is close to the occupied and another LMO is close to the virtual NTO (blue).

TABLE II. Percentage of "Laplace pairs" used in the excited state PNO construction for the HOMO-LUMO LE and CT transitions in a C_2H_4–C_2F_4 complex separated by 12 a.u. The excitation energy calculation was performed with the PNO-CIS(D)/cc-pVDZ model and different PNO truncation thresholds T_{PNO}.

$-\log(T_{\mathrm{PNO}})$	$C_2H_4 \rightarrow C_2H_4$	$C_2F_4 \rightarrow C_2F_4$	$C_2F_4 \rightarrow C_2H_4$	$C_2H_4 \rightarrow C_2F_4$
6	0.00	0.00	34.24	42.50
7	0.00	0.00	57.49	30.43
8	0.38	0.38	53.08	17.32
9	1.69	1.67	57.77	17.22
10	4.33	1.67	63.67	35.19

that $\alpha_{Lap} = 99$ and $\mathrm{T_{Lap}} = 100 \cdot \mathrm{T_{PNO}}$ is a reasonable choice.

For the determination of the parameters w_z and t_z for the Laplace transformation, the energy shift ω in the orbital denominator in Eq. (23) can have a non-negligible influence on the number of quadrature points that are needed to achieve a given accuracy. Particularly, this occurs for excitation energies of CT states computed with CIS(D). Here, ω_{CIS} often approaches the HOMO-LUMO gap. For efficiency reasons, we use for each state its own quadrature grid, which is optimized with the current estimate for the corresponding excitation energy to obtain a sufficient accuracy already with just a few quadrature points.

The accuracy of the numerical Laplace transformation is controlled by the mean squared error functional[56] $\sqrt{F^{Lap}}$, which is an approximate upper bound for the Laplace error in excitation energies. The error introduced by the numerical quadrature should not exceed the PNO truncation error, which can be roughly estimated by $\sqrt{T_{\mathrm{PNO}}}$ from the results of a benchmark set as shown below in Sec. VIII. To account for the fact that the numerical Laplace transformation is only applied to a set of selected pairs I_{Lap}, the threshold that controls the accuracy of the numerical quadrature is set to

$$\sqrt{F^{Lap}} \approx \frac{\sum_{ij} {}^{\mathrm{SOS}}\omega_{es}^{ij}}{\sum_{kl \in I_{Lap}} {}^{\mathrm{SOS}}\omega_{es}^{kl}} \sqrt{T_{\mathrm{PNO}}}. \tag{30}$$

With this automated selection of the pairs $kl \in I_{Lap}$ and $\sqrt{F^{Lap}}$ during the PNOs construction, we re-calculated the PNO truncation error for the $C_2H_4 - C_2F_4$ complex (see Fig. 2). For the LE states ($C_2H_4 \rightarrow C_2H_4$ and $C_2F_4 \rightarrow C_2F_4$), not more than 5% of the pairs were selected as shown in Table II. Conversely, for the CT states ($C_2F_4 \rightarrow C_2H_4$ and $C_2H_4 \rightarrow C_2F_4$), 15%–65% of the pairs were selected. The convergence of the total PNO truncation error in the CIS(D)/cc-pVDZ excitation energies for the four HOMO-LUMO excitations with the Laplace transformation applied to selected pairs during the ES-PNO construction is shown in Fig. 5. For all four states, we obtained truncation errors that are comparable to the mean absolute errors found previously for a benchmark set of organic chromophores with predominantly local excitations.[38]

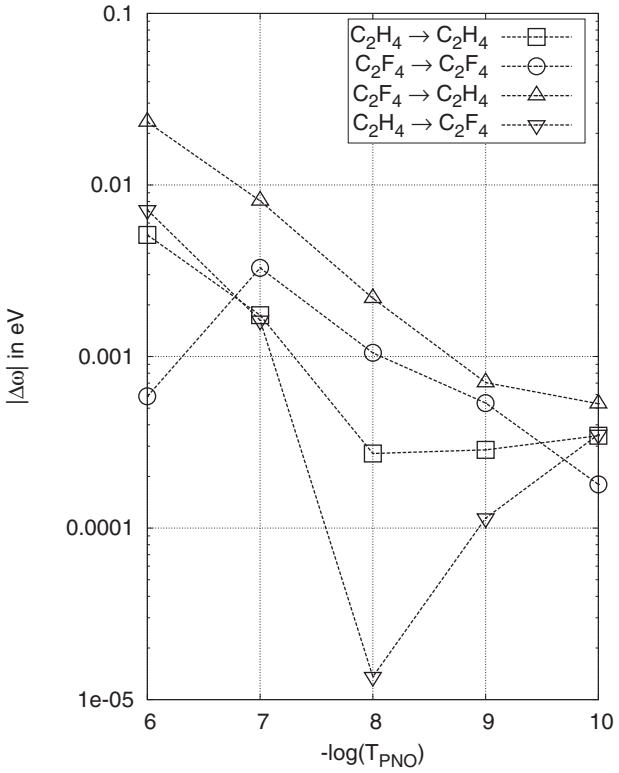


FIG. 5. PNO truncation errors of the total CIS(D)/cc-pVDZ excitation energy $|\Delta\omega|$ for HOMO-LUMO local and CT excitations with different PNO truncation thresholds T_{PNO} in a C_2H_4–C_2F_4 complex separated by 12 a.u. Numerical Laplace transformation was used for the PNO construction of selected pairs according to Eq. (30).

VI. SOLUTION OF THE EIGENVALUE PROBLEM WITH STATE-SPECIFIC PNO BASES

In CC response theory, the electronic excitation energies are the eigenvalues of the Jacobian **A**. For most applications, only a few of the lowest eigenpairs of **A** are of interest. Typically, these eigenpairs are determined iteratively with a Davidson-like algorithm.[57] The initial step of a standard Davidson algorithm is the computation of the reduced space Jacobian $A_{KL}^{red} = (b^K)^\dagger \mathbf{A} b^L = b^K \cdot \sigma^K$, where $K, L, \ldots$ enumerate the basis vectors b. Then, the eigenvalue problem is solved in the reduced space $\mathbf{A}^{red} U^f = \omega^f U^f$. The eigenvalues ω^f of $\mathbf{A}^{red}$ converge to the eigenvalues of **A** if the reduced space is successively expanded with new trial vectors b^K. With the eigenvalues ω^f and right eigenvectors U^f of $\mathbf{A}^{red}$, we can compute for selected states f the right eigenvectors $R^f = \mathbf{b} U^f$ and their residual vectors $\rho^f = \boldsymbol{\sigma} U^f - \omega^f R^f$ in the full space. The latter are used to terminate the algorithm if the residual norms $||\rho^f||$ are smaller than a convergence threshold. Moreover, the residual vectors are used to update the reduced space after they have been pre-conditioned and orthonormalized onto the previous trial vectors.

The introduction of truncated PNO expansions for the doubles trial vectors necessitates modifications of the standard Davidson procedure. First of all, the excited state PNOs depend on the physical character of the excited state. For single-excitation dominated transitions, they depend in particular on the eigenvalues and singles part of the

eigenvectors, which are not known before the eigenproblem is solved. A solution to this problem is to construct new PNOs from the current eigenvalue ω and singles eigenvector R_{μ_1} and to restart the Davidson procedure. The new doubles eigenvector R_{μ_2} is obtained right after re-constructing the PNOs by solving $(A_{\mu_2\nu_2} - \omega)R_{\nu_2} = -A_{\mu_2\nu_1}R_{\nu_1}$. For single-excitation dominated transitions, a criterion for the construction of new PNOs can be deduced from the overlap $R^{(0)} \cdot R$ of the initial $R^{(0)}$ and the current eigenvector R. If $1 - |R^{(0)} \cdot R|$ becomes much larger than the residual norm $||\rho||$, the error from an inappropriate PNO space is usually more severe than the reduced space incompleteness error of the Davidson algorithm, which is then restarted. Thus, we use as criterion for the generation of new PNOs the condition $1 - |R^{(0)} \cdot R| \geq \beta||\rho||$. Test calculations revealed that the best performance is roughly obtained with $\beta = 10$. The construction of new PNOs is, however, suppressed if the remaining error approaches the PNO truncation error, so that no further improvement can be expected from a new PNO construction. We estimate the PNO truncation error for excitation energies by $\sqrt{T_{\text{PNO}}}$.

A further complication emanates from the state-specific PNO expansions of the doubles part of the eigenvectors if several states are optimized simultaneously in a multi-state algorithm. Computing off-diagonal elements of the reduced space Jacobian $\mathbf{A}^{red}$ by a multi-state procedure requires, without introducing any further approximation, the $\mathbf{A}_{\mu_2\nu_2}$ block to be projected from the left and right onto different PNO bases. This leads to a quadratic scaling of the Jacobian right-transformations with the number of exited states, which would be inefficient.

A quadratic scaling could be avoided, if one would treat all states in a joint PNO basis. However, such a joint PNO basis depends rather on the number of selected states than on their individual character of excitation and increases as we increase the number of states that are simultaneously optimized. Especially, for large molecules, where electrons are excited from and into different chromophores of the molecule, it is expected that a merged PNO space increases drastically with the number of excited states and counteracts the compactness of state-specific PNO spaces.

For second-order methods for single-excitation dominated transitions, an alternative strategy, which also avoids the quadratic scaling, is to partition the eigenvalue equation and determine the eigenvalues of an effective Jacobian in the singles space only.[21] This is possible if a truncation is only applied to the doubles space. By following this strategy, the singles trial vectors are employed to compute the effective Jacobian in the reduced space. Moreover, the doubles trial vectors are part of the effective Jacobian itself and need to be determined in each iteration of the Davidson procedure either by solving a linear system of equations or by numerical Laplace transformation.[21] This strategy, however, cannot be extended efficiently to higher-order methods like CCSD or methods that describe also doubly excited states correctly through first order like the extended ADC(2) method.[41]

An approach that avoids this problem is to calculate the eigenpairs of the Jacobian one after the other with a single-state method. Such algorithms are suited for local methods, which employ state-specific local bases, but will usually require more iterations to optimize several states. Furthermore, degenerate states and complex roots can be a problem. Since the Davidson algorithm for a single state converges to the lowest eigenvalue in the subspace that can be visited by the trial vectors, the eigenvectors for the lower roots must be projected out to achieve convergence to higher roots, e.g., by using a rank-k modified Jacobian

$$\mathbf{A}^k = \mathbf{A} + \mu \sum_f^{k-1} R^f \, (L^f)^T. \tag{31}$$

The rank-k modified Jacobian $\mathbf{A}^k$ is constructed from the original Jacobian $\mathbf{A}$, a shift parameter μ, and the converged left L^f and right eigenvectors R^f of the previously determined roots. This technique is often called deflation[58] and goes back to the work of Hotelling[59] and Wielandt.[60] Deflation, as shown in Eq. (31), preserves all eigenvalues and eigenvectors of the un-deflated Jacobian apart from the previously determined $k - 1$ eigenpairs for which the eigenvalues are shifted by μ, but requires for the latter eigenpairs both left and right eigenvectors. For vertical excitation energies, where only the eigenvalues are required, it is sufficient to deflate $\mathbf{A}$ by $R^f(R^f)^T$, which preserves only the eigenvalues but does not require the left eigenvectors.

In the present PNO implementation, we assign each state its own PNO basis. In principle, this is problematic because we do not know the eigenvectors R^f of the previously optimized states f in the PNO basis of state k. To circumvent this problem in our PNO implementation, the Jacobian is deflated by eigenvectors that are projected from their own onto the current PNO basis $\mathbf{S}^{kf} R^f \mathbf{S}^{fk}$ with the overlap $\mathbf{S}^{fk}$ between the PNO bases for the states f and k. This projection preserves the eigenvalues within the limits that result from the truncated PNO expansions. The accuracy of the excitation energies is still controlled by the PNO threshold. To ensure that the Davidson algorithm does not converge to a previously determined eigenvalue again, the shift parameter μ has to be sufficiently large. We set μ to 1.5 times the CIS excitation energy for the highest eigenvalue that is optimized by the eigenvalue solver.

VII. COMPUTATIONAL DETAILS

The PNO approach for iterative second-order methods described in Secs. II–VI was implemented in a development version of the TURBOMOLE program package.[61] PNOs for ground as well as excited states with natural occupation numbers $n_{\bar{a}}^{ij}$ that are larger than a user-defined PNO threshold T_{PNO} are selected for the calculation. Additionally, pairs ij are excluded from the ground and excited state PNO construction if the SOS estimate for the pair energy ${}^{\text{SOS}}e_{\text{MP2}}^{ij}$ or ${}^{\text{SOS}}\omega_{es}^{ij}$, respectively, are smaller than a user-defined pair threshold T_{pair}. As in our previous study on PNO-CIS(D),[38] we set both thresholds to the same value in all calculations. Indeed, this leads to larger costs for the PNO construction. But, it ensures that the pair threshold does not affect the final results. To guarantee that the errors from the OSV approximation are negligible compared to the PNO truncation error, the threshold for

the OSV selection has been set to $0.1\,T_{\mathrm{PNO}}$. New PNOs for the Davidson procedure were only constructed if the overlap criterion $1 - |R^{(0)} \cdot R|$ was above $\sqrt{T_{\mathrm{PNO}}}$. For the current test calculations, we have conservatively set $\beta = 1$. Since, compared to other localization schemes, the Pipek-Mezey[62] procedure applied to the occupied MO space yields the most compact PNO spaces for excited states,[38] we chose this localization procedure in all our calculations. For iterative second-order methods, the CIS excitation energies and singles eigenvectors were initially employed for the ES-PNO construction and as singles trial vectors for the Davidson procedure.

The Hartree-Fock calculations have been performed with the dscf module,[63] DFT calculations with the ridft module,[64] and CIS(D) as well as CC2 calculations with the ricc2 module[43] of the TURBOMOLE program package[65] using the TZVP,[66] TZVP and def2-TZVPP,[67,68] cc-pVDZ and cc-pVTZ,[69] and aug-cc-pVTZ[70] orbital basis sets. For all DFT and correlated wave function calculations, we made use of the RI approximation for two-electron integrals using auxiliary basis sets from Refs. 46, 67, 68, 71, and 72, which are optimized for the corresponding orbital basis sets. Furthermore, all core electrons have been kept frozen, i.e., $1s^2$ for C, N, and O atoms and $1s^2 2s^2 2p^6$ for S and Cl atoms.

The structures for the benchmark set developed by Schreiber *et al.* and for 2,4-dichloro-6-[p-(N,N-diethylamino)biphenylyl]-1,3,5-triazine (DBQ) were taken from the supplementary material of Refs. 73 and 74. The structure of the phenothiazine-isoalloxazine-pyrene triad was kindly provided by the authors of Ref. 20. The structures of C_2H_4, C_2F_4, and terrylenediimide[75] were optimized at the DFT/B3LYP level with the def2-TZVP basis set. After separate geometry optimizations, C_2H_4 and C_2F_4 were stacked on top of each other with a distance of 12 a.u. The structures obtained from geometry optimizations as well as the structures of the glycine chains with standardized parameters for internal coordinates are provided in the supplementary material.[76]

VIII. RESULTS AND DISCUSSION

A. Accuracy of the eigenvalue solver with state-specific PNOs

Similar to our previous study on PNO-CIS(D), we investigated the PNO truncation errors for the CC2 model by computing excitation energies of 28 organic molecules that are part of the benchmark set from Ref. 73. For the 142 singlet excited states described in Ref. 77, we included all states for the TZVP basis, however, excluded the two highest excited states of both naphthalene and pyrazine computed with the aug-cc-pVTZ basis set. For these highly excited states, the PNO truncation errors are for $-\log(T_{\mathrm{PNO}}) = 6, 7$ of the same order as the energy differences between the highest states so that no definite assignment was possible.

Figs. 6 and 7 show for these two test sets the mean absolute errors (MAE) and the maximum errors (MAX) of both the iterative PNO-CC2 and the non-iterative PNO-CIS(D) method[38] for $-\log(T_{\mathrm{PNO}}) = 6, \ldots, 9$. The results for PNO-CIS(D) are taken from Ref. 38 and are obtained for a subset

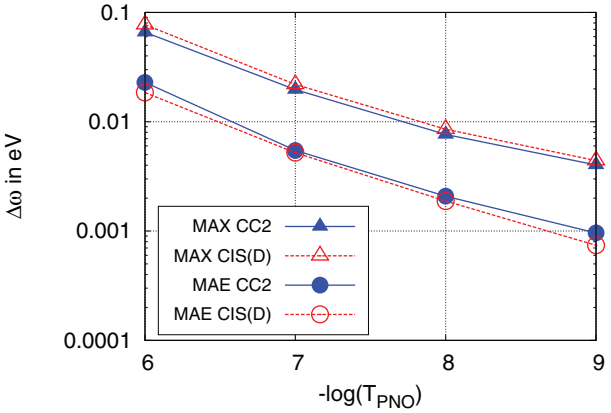


FIG. 6. Convergence of the truncation errors $\Delta\omega$ for PNO-CIS(D)/TZVP and PNO-CC2/TZVP. For details of the test, set see text. MAX is the maximum and MAE the mean absolute error.

of the benchmark set of Schreiber *et al.*[73] In Ref. 38, only those states were included where the CIS eigenvectors have a substantial overlap with the eigenvector from CC2 so that a comparison with the latter method was possible. Figs. 6 and 7 demonstrate how MAX and MAE for PNO-CC2 and PNO-CIS(D) decrease with T_{PNO}. Both statistical measures are very similar for the iterative PNO-CC2 and non-iterative PNO-CIS(D) method. This is also the case if for PNO-CC2 the statistical measures are calculated for the same subset of states like for PNO-CIS(D). Thus, compared to the perturbative PNO-CIS(D) method, the additional errors due to only incomplete self-consistency of the excited state PNOs and the projection error in the deflation of the Jacobian are minor. Overall, the accuracy of the PNO approach as proposed for non-iterative PNO-CIS(D) transfers to iterative second-order methods.

B. Performance of the PNO implementation

In a previous publication, Hättig *et al.*[32] proposed a hybrid OSV-PNO approach for MP2 and MP3 and their explicitly correlated F12 variants. It was concluded that relating the OSV truncation threshold to the PNO threshold by $T_{\mathrm{OSV}} = 0.1\,T_{\mathrm{PNO}}$ increases the truncation errors only

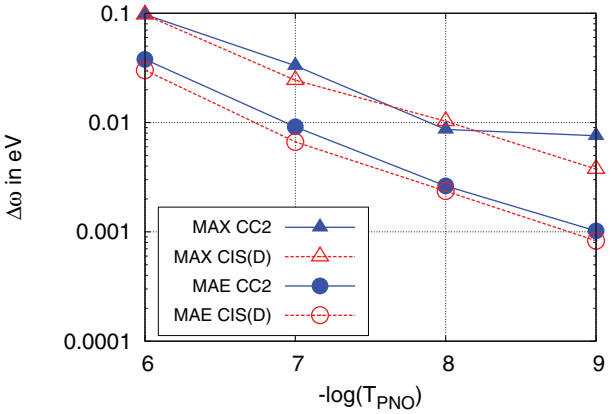


FIG. 7. Convergence of the truncation errors $\Delta\omega$ for PNO-CIS(D)/aug-cc-pVTZ and PNO-CC2/aug-cc-pVTZ. For details of the test, set see text. MAX is the maximum and MAE the mean absolute error.

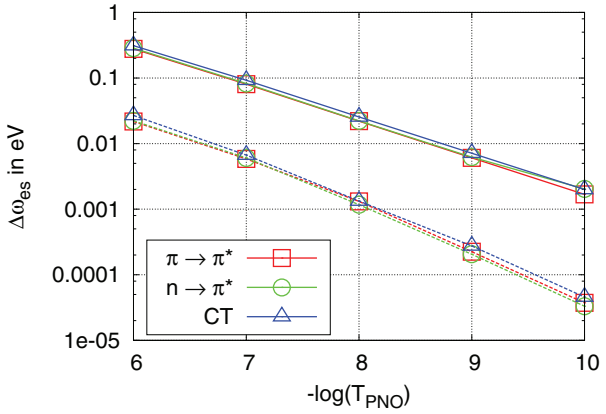


FIG. 8. Total truncation errors (solid line) for the hybrid OSV-PNO approach and OSV truncation errors (dashed line) of ω_{es} in CIS(D)/def2-TZVPP calculations for S_1 ($\pi \rightarrow \pi^*$), S_4 ($n \rightarrow \pi^*$), and S_8 (CT) of DBQ.

insignificantly so that the accuracy of the PNO calculation is still fully determined by the PNO threshold. In the current work, we examined if this transfers to excitation energy calculations. In Fig. 8, the additional error from the OSV approximation is compared to the total truncation error for ω_{es} with the hybrid OSV-PNO approach for a $\pi \rightarrow \pi^*$, a $n \rightarrow \pi^*$, and a CT excitation in DBQ. Independent from the character of the excitation, the additional errors introduced by the OSV approximation are with $T_{\mathrm{OSV}} = 0.1\,T_{\mathrm{PNO}}$ more than one order of magnitude smaller than the PNO truncation error. Thus, like for the ground state energy, $T_{\mathrm{OSV}} = 0.1\,T_{\mathrm{PNO}}$ is also for excitation energies sufficient to keep the OSV truncation error negligible.

For the present $\mathcal{O}(\mathcal{N}^4)$-scaling PNO-CC2 as well as for the $\mathcal{O}(\mathcal{N}^5)$-scaling RI-CC2 implementation, we investigated the costs as function of the number of AO basis functions N for linear glycine chains $(\mathrm{gly})_{2^k}$ for $k = 0, 1, 2, 3, 4$ with the cc-pVDZ and the aug-cc-pVTZ basis sets. The timings for an evaluation of the CC vector function and a Jacobian transformation are shown in Fig. 9 for the cc-pVDZ and in Fig. 10 for the aug-cc-pVTZ basis set. If only these costs are considered,

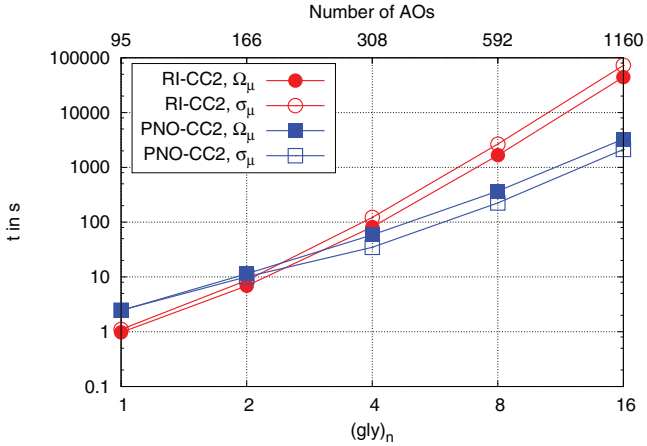


FIG. 9. Timings for the computation of the CC vector function Ω_μ and the Jacobian transformation σ_μ for the lowest excited state of glycine chains $(\mathrm{gly})_{2^k}$ with $k = 0, 1, \ldots, 4$ with RI-CC2 and PNO-CC2 ($T_{\mathrm{PNO}} = 10^{-8}$) in the cc-pVDZ basis set.

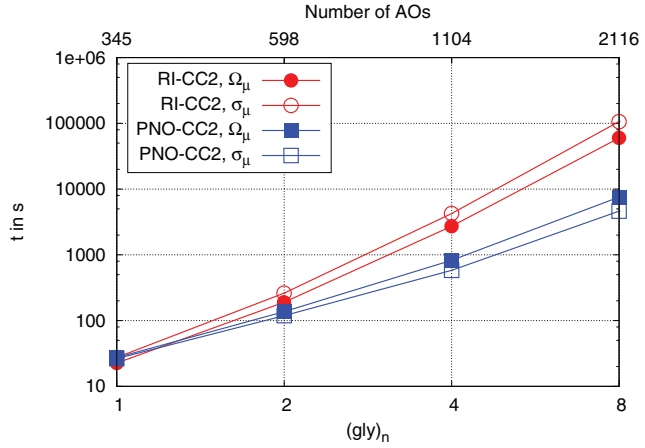


FIG. 10. Timings for the computation of the CC vector function Ω_μ and the Jacobian transformation σ_μ for the lowest excited state of glycine chains $(\mathrm{gly})_{2^k}$ with $k = 0, 1, \ldots, 3$ with RI-CC2 and PNO-CC2 ($T_{\mathrm{PNO}} = 10^{-8}$) in the aug-cc-pVTZ basis set.

the preliminary PNO-CC2 implementation is already faster than RI-CC2 for $(\mathrm{gly})_4$ with the cc-pVDZ and for $(\mathrm{gly})_2$ with the aug-cc-pVTZ basis set. We note, however, that the approximate self-consistent determination of the PNOs together with the single-state Davidson algorithm leads to a larger number of iterations for converging the excitation energies. In the canonical RI-CC2 implementation, the Jacobian transformations are more time-consuming than the computation of the vector function due to the additional computational overhead for the computation of $\bar{K}^{ij}_{ab}$ in comparison to $\hat{K}^{ij}_{ab}$. The Jacobian transformations in the PNO implementation is, in contrast to this, less costly than the evaluation of the vectors function because the PNO expansions for the excited states is more compact than for the ground state. For the computation of the Jacobian transformations, the effective cost-scaling estimated from the timings for the largest peptides in Fig. 10 is $N^{3.3}$ ($N^{4.9}$ in RI-CC2) for the cc-pVDZ and $N^{3.2}$ ($N^{5.0}$ in RI-CC2) for the aug-cc-pVTZ basis set. For the Jacobian transformation in PNO-CC2, more than 96% of the time is spend for the computation of the intermediates that are needed for the σ^{JG} and σ^{H} terms, which have in the current implementation still cubic and quartic cost-scalings with sizeable pre-factors. For the largest peptides computed in the respective basis set, the timings for the Jacobian transformations are already with the preliminary PNO-CC2 implementation nevertheless even a factor of 5 smaller than with the quartically scaling LT-SOS-CC2 implementation presented in Ref. 56.

In our previous study on PNO expansions for excited states, we compared the convergence of the truncation errors of a LE (S_5 in CIS(D), S_4 in CIS) and a CT state (S_1 in CIS(D), S_7 in CIS) in the phenothiazine-isoalloxazine-pyrene triad. For the CT state, the excited state contribution ω_{es} to the (D) doubles correction showed a considerable slower convergence with the PNO threshold than for the LE state. This problem has now been resolved with the Laplace transformation to improve the PNOs for excited states as demonstrated in Fig. 11. Without applying the Laplace transformation, the truncation errors for the LE and CT state differ significantly, up to one order of magnitude for $T_{\mathrm{PNO}} = 10^{-10}$. Replacing the

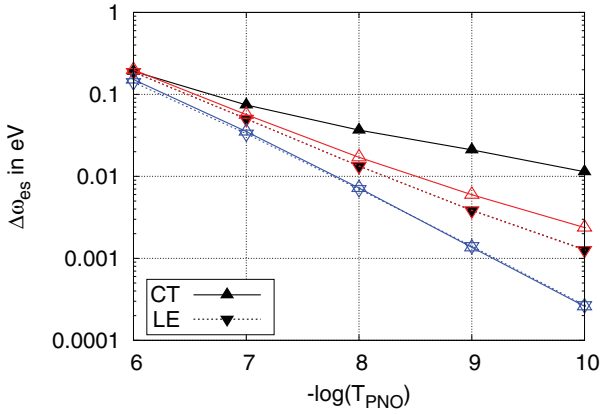


FIG. 11. PNO truncation errors of ω_{es} in CIS(D)/cc-pVDZ calculations for S_1 (CT) and S_5 (LE) of the triad (see text) with different PNO truncation thresholds T_{PNO}. Numerical Laplace transformation was used for the PNO construction of no (black), according to Eq. (30) selected (red), or all pairs (blue).

diagonal approximation for all pairs by the Laplace transformation yields almost identical truncation errors for both the LE and CT state. If "Laplace pairs" are selected according to Eq. (30), we still obtain a significant error reduction for ω_{es} of the CT state. This results in very similar PNO truncation errors for the total CIS(D) excitation energy of the LE and CT state (see Fig. 12).

We investigated furthermore the performance of the PNO-CC2 method for a typical application: a large organic molecule with a ground-state electronic structure that can be qualitatively described by a single configuration. We computed the lowest vertical excitation energies of terrylenediimide,[75] which is a fluorescent dye with high extinction coefficients and quantum yields. For the ground state and the five lowest excited states, we listed in Table III the average number of OSVs per LMO and the relative dimension of the pre-PNO as well as of the PNO doubles space compared to the full doubles space. The number of OSVs is for all excited states approx. 20% larger than for the ground state. This correlates with the relative dimension of the pre-PNO doubles

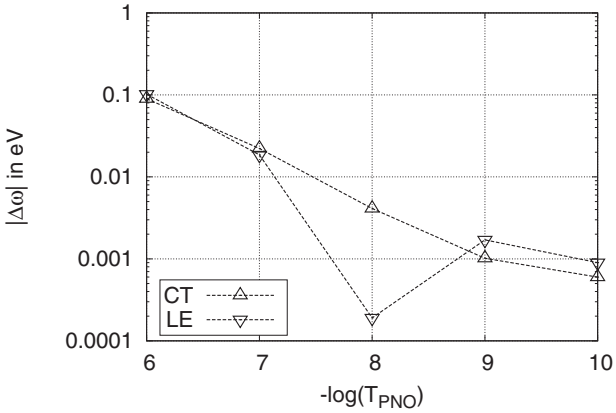


FIG. 12. Absolute PNO truncation errors $|\Delta\omega|$ of CIS(D)/cc-pVDZ for S_1 (CT) and S_5 (LE) of the triad (see text) with different PNO truncation thresholds T_{PNO}. Numerical Laplace transformation was used for the PNO construction of selected pairs as described in Eq. (30).

TABLE III. Average number of selected OSVs per LMO N_{OSV} ($T_{\mathrm{OSV}} = 10^{-9}$) and relative size of both the pre-PNO ($T_{\mathrm{OSV}} = 10^{-9}$) and PNO doubles space ($T_{\mathrm{PNO}} = 10^{-8}$) for the PNO-CC2/cc-pVDZ calculation on terrylenediimide (156 active occupied and 906 canonical virtual orbitals).

			Dimension relative to full space in %	
State	ω (in eV)	N_{OSV}	Pre-PNO	PNO
S_0	–	80	3.1	0.082
S_1	2.17	95	3.9	0.051
S_2	3.38	97	4.1	0.051
S_3	3.19	96	3.9	0.050
S_4	3.44	93	3.4	0.045
S_5	3.58	94	3.6	0.046

spaces, which are for the excited states 10%–30% larger than for the ground state. Enlarged OSV spaces for excited states are expected because the excited state OSVs must be suitable to approximate $\hat{B}^Q_{ai}$ and $\bar{B}^Q_{ai}$ and not only $\hat{B}^Q_{ai}$ like the ground state OSVs. The excited state PNO spaces for the doubles are, however, approximately 40% smaller than for the ground states. From the discussion of Sec. V, it is clear that only pairs with at least one LMO involved in the electronic transition have sizeable exchange integrals $\bar{K}^{ij}_{ab}$ and contribute to the excited state PNO expansion. For a PNO-CC2/cc-pVDZ ($T_{PNO} = 10^{-8}$) calculation for terrylenediimide with 156 correlated electrons and 1126 basis functions, the doubles space for ground and excited states is compressed by more than a factor of 1000. The OSV approximation alone without subsequent PNO selection would, in contrast to this, reduce the doubles space only by a factor of ≈30.

IX. CONCLUSION

We presented a PNO implementation for non-perturbative excited state second-order methods. The extension of the hybrid OSV-PNO ansatz proposed recently for ground state PNOs has been generalized to the excited state PNOs with only minor modifications in the OSV generation. The accuracy of the initial PNO method is retained and exclusively controlled by the PNO truncation threshold. This paves the way for a quadratically scaling PNO implementation which employs an iterative determination of OSVs and a local RI approximation as described for PNO-MP2 in Ref. 47.

Furthermore, we analyzed and resolved the slower convergence of the PNO truncation error for charge-transfer excited states. For these states, a considerable number of pairs have only few PNOs with significant energy contributions. For these pairs, the PNOs are more sensitive to the neglect of the off-diagonal elements in the Fock matrix during their construction. A numerical Laplace transformation of the orbital energy denominators for selected pairs during the excited state PNO construction of charge-transfer states resolves this problem and leads to a similar accuracy for CT and local excitations.

The eigenvalue problem with state-specific truncated PNO expansions can be solved by combining the Davidson

algorithm with deflation to project out roots that have already been determined and an automated refresh with a generation of new PNOs to achieve an approximate self-consistency of the PNO space. The procedure has been validated for PNO-CC2 by applying it to a test set that contains more than 140 excited states in 28 organic molecules. The truncation errors of PNO-CC2 are only slightly larger than for the perturbative CIS(D) method.

The computational efficiency of the approach is demonstrated for the terrylenediimide molecule and a series of glycine oligomers. Even with a conservative PNO threshold of 10^{-8}, we obtained a reduction of the doubles space compared to a canonical calculation by a factor of 1000 for terrylenediimide. This compression is even more pronounced for excited states than for the ground state and typically a factor of 30 higher than in an OSV calculation without subsequent PNO construction. Already in the current preliminary implementation, we have shown for the glycine oligomers that the approach has an early break even point with a canonical RI-CC2 implementation between 100 and 300 basis functions and outperforms quartically scaling Laplace-transformed SOS-CC2, even though the same-spin exchange correlation contribution is fully included. These results encourage further developments that cover, first, the reduction of the scaling to $\mathcal{O}(\mathcal{N}^2)$ to enable calculations with up to 10 000 basis functions and, second, the extension of the excited state PNO methodology to higher-order methods like extended ADC(2)-x or CCSD.

ACKNOWLEDGMENTS

Financial support by the Deutsche Forschungsgemeinschaft (DFG) through Grant No. HA/2588-7 is gratefully acknowledged.

[1] O. Christiansen, H. Koch, and P. Jørgensen, Chem. Phys. Lett. **243**, 409 (1995).
[2] H. Koch, O. Christiansen, P. Jørgensen, A. S. de Merás, and T. Helgaker, J. Chem. Phys. **106**, 1808 (1997).
[3] O. Christiansen, H. Koch, and P. Jørgensen, J. Chem. Phys. **103**, 7429 (1995).
[4] M. Kállay and J. Gauss, J. Chem. Phys. **121**, 9257 (2004).
[5] K. Andersson, P.-Å. Malmqvist, and B. O. Roos, J. Chem. Phys. **96**, 1218 (1992).
[6] E. Runge and E. K. U. Gross, Phys. Rev. Lett. **52**, 997 (1984).
[7] E. K. U. Gross and W. Kohn, Phys. Rev. Lett. **55**, 2850 (1985).
[8] A. Dreuw and M. Head-Gordon, Chem. Rev. **105**, 4009 (2005).
[9] M. Häser, Theor. Chim. Acta **87**, 147 (1993).
[10] D. S. Lambrecht, B. Doser, and C. Ochsenfeld, J. Chem. Phys. **123**, 184102 (2005).
[11] H. Stoll, Chem. Phys. Lett. **191**, 548 (1992).
[12] J. Friedrich, M. Hanrath, and M. Dolg, J. Phys. Chem. **126**, 154110 (2007).
[13] R. A. Mata and H. Stoll, J. Chem. Phys. **134**, 034122 (2011).
[14] P. Pulay, Chem. Phys. Lett. **100**, 151 (1983).
[15] S. Saebø and P. Pulay, Annu. Rev. Phys. Chem. **44**, 213 (1993).
[16] M. Schütz, G. Hetzer, and H.-J. Werner, J. Chem. Phys. **111**, 5691 (1999).
[17] M. Schütz and H.-J. Werner, Chem. Phys. Lett. **318**, 370 (2000).
[18] M. Schütz and H.-J. Werner, J. Chem. Phys. **114**, 661 (2001).
[19] T. Korona and H.-J. Werner, J. Chem. Phys. **118**, 3006 (2003).
[20] D. Kats, T. Korona, and M. Schütz, J. Chem. Phys. **125**, 104106 (2006).
[21] D. Kats and M. Schütz, J. Chem. Phys. **131**, 124117 (2009).
[22] W. Meyer, Int. J. Quantum Chem. **5**, 341 (1971).
[23] W. Meyer, Theor. Chim. Acta **35**, 277 (1974).
[24] R. Ahlrichs and F. Driessler, Theor. Chim. Acta **36**, 275 (1975).
[25] R. Ahlrichs, H. Lischka, V. Staemmler, and W. Kutzelnigg, J. Chem. Phys. **62**, 1225 (1975).
[26] F. Neese, F. Wennmohs, and A. Hansen, J. Chem. Phys. **130**, 114108 (2009).
[27] F. Neese, A. Hansen, and D. G. Liakos, J. Chem. Phys. **131**, 064103 (2009).
[28] O. Vahtras, J. Almlöf, and M. Feyereisen, Chem. Phys. Lett. **213**, 514 (1993).
[29] M. Feyereisen, G. Fitzgerald, and A. Komornicki, Chem. Phys. Lett. **208**, 359 (1993).
[30] D. Tew, B. Helmich, and C. Hättig, J. Chem. Phys. **135**, 074107 (2011).
[31] D. P. Tew and C. Hättig, Int. J. Quantum Chem. **113**, 224 (2013).
[32] C. Hättig, D. P. Tew, and B. Helmich, J. Chem. Phys. **136**, 204105 (2012).
[33] J. Yang, G. K.-L. Chan, F. R. Manby, M. Schütz, and H.-J. Werner, J. Chem. Phys. **136**, 144105 (2012).
[34] J. Yang, Y. Kurashige, F. R. Manby, and G. K. L. Chan, J. Chem. Phys. **134**, 044123 (2011).
[35] Y. Kurashige, J. Yang, G. K.-L. Chan, and F. R. Manby, J. Chem. Phys. **136**, 124106 (2012).
[36] C. Riplinger and F. Neese, J. Chem. Phys. **138**, 034106 (2013).
[37] C. Krause and H.-J. Werner, Phys. Chem. Chem. Phys. **14**, 7591 (2012).
[38] B. Helmich and C. Hättig, J. Chem. Phys. **135**, 214106 (2011).
[39] M. Head-Gordon, R. J. Rico, M. Oumi, and T. J. Lee, Chem. Phys. Lett. **219**, 21 (1994).
[40] M. Head-Gordon, M. Oumi, and D. Maurice, Mol. Phys. **96**, 593 (1999).
[41] J. Schirmer, Phys. Rev. A **26**, 2395 (1982).
[42] C. Hättig, Adv. Quantum Chem. **50**, 37 (2005).
[43] C. Hättig and F. Weigend, J. Chem. Phys. **113**, 5154 (2000).
[44] H. Koch, A. S. de Merás, T. Helgaker, and O. Christiansen, J. Chem. Phys. **104**, 4157 (1996).
[45] T. Helgaker, P. Jørgensen, and J. Olsen, *Molecular Electronic-Structure Theory* (Wiley, New York, 2000).
[46] F. Weigend, A. Köhn, and C. Hättig, J. Chem. Phys. **116**, 3175 (2002).
[47] G. Schmitz, B. Helmich, and C. Hättig, Mol. Phys. 1 (2013).
[48] L. D. Lathauwer, B. D. Moor, and J. Vandewalle, SIAM J. Matrix Anal. Appl. **21**, 1253 (2000).
[49] K. Inoue and K. Urahama, Electron. Commun. Jpn., Part 2: Electron. **90**, 42 (2007).
[50] J. Almlöf, Chem. Phys. Lett. **181**, 319 (1991).
[51] M. Häser and J. Almlöf, J. Chem. Phys. **96**, 489 (1992).
[52] A. Dreuw, J. L. Weisman, and M. Head-Gordon, J. Chem. Phys. **119**, 2943 (2003).
[53] A. V. Luzanov, A. A. Sukhorukov, and V. É. Umanskii, Theor. Exp. Chem. **10**, 354 (1976).
[54] R. L. Martin, J. Chem. Phys. **118**, 4775 (2003).
[55] V denotes the full rank of $\bar{K}_{ab}^{ij}$ for a given pair ij. This can be the number of either canonical virtual orbitals or pre-PNOs.
[56] N. O. C. Winter and C. Hättig, J. Chem. Phys. **134**, 184101 (2011).
[57] E. R. Davidson, J. Comput. Phys. **17**, 87 (1975).
[58] Y. Saad, *Numerical Methods for Large Eigenvalue Problems*, 2nd ed. (Society of Industrial and Applied Mathematics, 2011).
[59] H. Hotelling, J. Educ. Psychol. **24**, 417 (1933).
[60] H. Wielandt, Beiträge zur mathematischen Behandlung komplexer Eigenwertprobleme, Teil V: Bestimmung höherer Eigenwerte durch gebrochene Iteration, Bericht B 44/J/37, Aerodynamische Versuchsanstalt Göttingen, 1944 (11 pages).
[61] TURBOMOLE development version, 2013, see http://www.turbomole.com.
[62] J. Pipek and P. G. Mezey, J. Chem. Phys. **90**, 4916 (1989).
[63] M. Häser and R. Ahlrichs, J. Comput. Chem. **10**, 104 (1989).
[64] O. Treutler and R. Ahlrichs, J. Chem. Phys. **102**, 346 (1995).
[65] TURBOMOLE V6.4 2012, a development of University of Karlsruhe and Forschungszentrum Karlsruhe GmbH, 1989–2007, TURBOMOLE GmbH, since 2007; available from http://www.turbomole.com, 2012.
[66] A. Schäfer, C. Huber, and R. Ahlrichs, J. Chem. Phys. **100**, 5829 (1994).
[67] F. Weigend, M. Häser, H. Patzelt, and R. Ahlrichs, Chem. Phys. Lett. **294**, 143 (1998).
[68] F. Weigend and R. Ahlrichs, Phys. Chem. Chem. Phys. **7**, 3297 (2005).
[69] T. H. Dunning, J. Chem. Phys. **90**, 1007 (1989).
[70] R. A. Kendall, T. H. Dunning, and R. J. Harrison, J. Chem. Phys. **96**, 6796 (1992).
[71] K. Eichkorn, F. Weigend, O. Treutler, and R. Ahlrichs, Theor. Chem. Acc. **97**, 119 (1997).
[72] F. Weigend, Phys. Chem. Chem. Phys. **8**, 1057 (2006).

[73]M. Schreiber, M. R. Silva-Junior, S. P. A. Sauer, and W. Thiel, J. Chem. Phys. **128**, 134110 (2008).
[74]L. Goerigk and S. Grimme, J. Chem. Phys. **132**, 184103 (2010).
[75]F. O. Holtrup, G. R. J. Müller, H. Quante, S. De Feyter, F. C. De Schryver, and K. Müllen, Chem.-Eur. J. **3**, 219 (1997).
[76]See supplementary material at http://dx.doi.org/10.1063/1.4819071 for input structures of the C_2H_4–C_2F_4 complex, terrylenediimide, and glycine oligomers.
[77]M. R. Silva-Junior, S. P. Sauer, M. Schreiber, and W. Thiel, Mol. Phys. **108**, 453 (2010).